

Kinetic model of DNA replication in eukaryotic organisms

John Herrick¹, John Bechhoefer^{2*}, Aaron Bensimon^{1*}

¹*Laboratoire de Biophysique de l'ADN, Département des Biotechnologies, Institut Pasteur, 25-28, rue du Dr. Roux, 75724 Paris Cedex 15, France*

²*Department of Physics, Simon Fraser University, Burnaby, British Columbia, V5A 1S6, Canada*

**To whom correspondence should be addressed. E-mail: johnb@sfu.ca (J.B.) and abensim@pasteur.fr (A.B.)*

We formulate a kinetic model of DNA replication that quantitatively describes recent results on DNA replication in the *in vitro* system of *Xenopus laevis* prior to the mid-blastula transition. The model describes well a large amount of different data within a simple theoretical framework. This allows one, for the first time, to determine the parameters governing the DNA replication program in a eukaryote on a genome-wide basis. In particular, we have determined the frequency of origin activation in time and space during the cell cycle. Although we focus on a specific stage of development, this model can easily be adapted to describe replication in many other organisms, including budding yeast.

Although the organization of the genome for DNA replication varies considerably from species to species, the duplication of most eukaryotic genomes shares a number of common features:

- 1) DNA is organized into a sequential series of replication units, or replicons, each of which contains a single origin of replication (Hand, 1978; Friedman et al., 1997).
- 2) Each origin is activated not more than once during the cell-division cycle.
- 3) DNA synthesis propagates at replication forks bidirectionally from each origin (Cairns, 1963).
- 4) DNA synthesis stops when two newly replicated regions of DNA meet.

Understanding how these parameters are coordinated during the replication of the genome is essential for elucidating the mechanism by which *S*-phase is regulated in eukaryotic cells. In this article, we formulate a stochastic model based on these observations that yields a mathematical description of the process of DNA replication and provides a convenient way to use the full statistics gathered in any particular replication experiment. It allows one to deduce accurate values for the parameters that regulate DNA replication in the *Xenopus laevis* replication system, and it can be generalized to describe replication in any other eukaryotic system. This type of model has also been shown to apply for the case of RecA polymerizing on a single molecule of DNA (Shivashankar et al, 1999). The model turns out to be formally equivalent to a well-known stochastic description of the kinetics of crystal growth, which allows us to draw on a number of previously derived results and, perhaps equally important, suggests a vocabulary that we find useful and intuitive for understanding the process of replication.

KINETIC MODEL OF DNA REPLICATION

In the 1930s, several scientists independently derived a stochastic model that described the kinetics of crystal growth (Kolmogorov, 1937; Johnson and Mehl, 1939; Avrami, 1939). The “Kolmogorov-Johnson-Mehl-Avrami” (KJMA) model has since been widely used by metallurgists and other scientists to analyze thermodynamic phase transformations (Christian, 1981).

In the KJMA model, freezing kinetics result from three simultaneous processes:

- 1) nucleation, which leads to discrete solid domains.
- 2) growth of the domain.
- 3) coalescence, which occurs when two expanding domains merge.

Each of these processes has an analog in DNA replication in higher eukaryotes, and more specifically embryos:

- 1) The activation of an origin of replication is analogous to the nucleation of the solid domains during crystal growth.
- 2) Symmetric bidirectional DNA synthesis initiated (nucleated) at the origin corresponds to solid-domain growth.
- 3) Coalescence in crystal growth is analogous to multiple dispersed sites of replicating DNA (replication fork) that advance from opposite directions until they merge.

In the simplest form of the KJMA model, solids nucleate anywhere in the liquid, with equal probability for all spatial locations (“homogeneous nucleation”), although it is straightforward to describe nucleation at pre-specified sites (“heterogeneous nucleation”), which would

correspond to a case where replication origins are specified by fixed genetic sites along the genome. Once a solid domain has been nucleated, it grows out as a sphere at constant velocity v . When two solid domains impinge, growth ceases at the point of contact, while continuing elsewhere. KJMA used elementary methods to calculate quantities such as $f(\tau)$, the fraction of the volume that has crystallized by time (τ). Much later, more sophisticated methods were developed to describe the detailed statistics of domain sizes and spacings (Sekimoto, 1991; Ben-Naim and Krapivsky, 1996).

DNA replication, of course, corresponds to one-dimensional crystal growth; the shape in three dimensions of the one-dimensional DNA strand does not directly affect the kinetics modeling. (In the model, replication is one dimensional along the DNA. The configuration of DNA in three dimensions is not directly relevant to the model but can enter indirectly via the nucleation function $I(x, \tau)$. For example, if, for steric reasons, certain regions of the DNA are inaccessible to replication factories, those regions would have a lower (or even zero) value of I .) The one-dimensional version of the KJMA model assumes that domains grow out at velocity v , assumed to remain constant. The nucleation rate $I(x, \tau) = I_0$ is defined to be the probability of domain formation per unit length of unreplicated DNA per unit time, at the position x and time τ . Following the analogy to the one-dimensional KJMA model, we can calculate the kinetics of DNA replication during S -phase. This requires determining the fraction of the genome $f(\tau)$ that has already been replicated at any given moment during S -phase. One finds

$$f(\tau) = 1 - e^{-I_0 v \tau^2}, \quad (1)$$

which defines a sigmoidal curve. (Eq. 1 assumes an infinite genome length. The relative importance of the finite size of chromosomes is set by the ratio (fork velocity * duration of S -phase) / chromosome length (Cahn, 1996). In the case of the experiment analyzed in this paper, this ratio is ≈ 10 bases/sec * 1000 sec / 10^7 bases/chromosome $\approx 10^{-3}$, which we neglect.)

A more complete description of replication kinetics requires detailed analysis of different statistical quantities, including measurements made on replicated regions (eyes), unreplicated regions (holes), and eye-to-eye sizes (the eye-to-eye size is defined as the length between the center of one eye and the center of a neighboring eye.) The probability distributions may be expressed as functions either of time τ or replicated fraction f . For example, the distribution of holes of size ℓ at time τ , $\rho_h(\ell, \tau)$ can be derived by a simple extension of the argument leading to Eq. 1:

$$\rho_h(\ell, \tau) = I_0 \tau \cdot e^{-I_0 \tau \ell}. \quad (2)$$

From Eq. 2, the mean size of holes at time τ is

$$\ell_h(\tau) = \frac{1}{I_0 \tau}. \quad (3)$$

Determining the probability distributions of replicated lengths (eye sizes) is complicated because a given replicated length may come from a single origin or it may result from the merger of two or more replicated regions. Thus, one must calculate in effect an infinite number of probabilities; by contrast, holes of a given length arise in only one way (Ben-Naim and Krapivsky, 1996). One can nonetheless derive a simple expression for $\ell_i(\tau)$, the mean replicated length at time τ , from a “mean-field” hypothesis (Plischke and Bergersen, 1994): the probability distribution of a given replicated length is assumed to be independent of the actual size of its neighbor. One can show that this mean-field hypothesis must always be true in one-dimensional growth problems, but not necessarily in the ordinary three-dimensional setting of crystal growth (Suckjoon Jun, private communication). In particular, if $I(\tau)$ depends on space, one expects correlations to be important. Using the mean-field hypothesis, we find

$$\ell_i(\tau) = \ell_h(\tau) \frac{f}{1-f} = \frac{e^{I_0 v \tau^2} - 1}{I_0 \tau} \quad (4)$$

and

$$\ell_{i2i}(\tau) = \ell_i(\tau) + \ell_h(\tau) = \frac{\ell_h(\tau)}{1-f} = \frac{e^{I_0 v \tau^2}}{I_0 \tau}. \quad (5)$$

These expressions for $\ell_i(\tau)$ and $\ell_{i2i}(\tau)$ allow one to collapse the experimental observations of ℓ_h , ℓ_i , and ℓ_{i2i} (the mean eye-to-eye separation) onto a single curve. (See Fig. 3D, below.)

Finally, we can calculate the average distance between origins of replication that were activated at different times during the replication process, which is just the inverse of I_{tot} , the time-integrated nucleation probability per unit length:

$$\ell_0 \equiv I_{tot}^{-1} = \frac{2}{\sqrt{\pi}} \cdot \sqrt{\frac{v}{I_0}} \quad (6)$$

The last expression shows that, as might have been guessed by dimensional analysis of the model parameters (I_0 and v), the basic length scale in the model is set by $\ell^* \equiv \sqrt{v/I_0}$.

Since the kinetics of DNA replication in any cell system depends on two fundamental parameters, replication fork velocity and initiation frequency, one of the principal goals of this kind of analysis is to derive accurate values for these parameters, along with inferences about any variation during the course of S -phase. As replicon size and the duration of S -phase depend on the values of these parameters, this information is indispensable for understanding the mechanisms regulating S -phase in

any given cell system (Pierron and Benard, 1996; Walter and Newport, 1997; Hyrien and Mechali, 1993; Coverly and Laskey, 1994; Blow and Chong, 1996; Shinomiya and Ina, 1991; Brewer and Fangman, 1993; Gomez and Anquera, 1999).

APPLICATION OF THE KJMA MODEL TO DNA REPLICATION IN *X. LAEVIS*

Recent experimental results obtained on the kinetics of DNA replication in the well-characterized *Xenopus laevis* cell-free system were used here to derive parameter values for that particular system. In those experiments, fragments of DNA that have completed one cycle of replication are stretched out on a glass surface using molecular combing (Bensimon et al., 1994; Michalet et al., 1997; Herrick et al., 1999). The DNA that has replicated prior to some chosen time t is labeled with a single fluorescent dye, while DNA that replicated after that time is labeled with two dyes. The result is a series of samples, each of which corresponds to a different time t during S -phase. Using an optical microscope, one can directly measure eye, hole, and eye-to-eye lengths at that time. We can thus monitor the evolution of genome duplication from time point to time point, as DNA synthesis advances. (See Fig. 1.)

Cell-free extracts of eggs from *Xenopus laevis* support the major transitions of the eukaryotic cell cycle, including complete chromosome replication under normal cell-cycle control and offers the opportunity to study the way that DNA replication is coordinated within the cell cycle. In the experiment, cell extract was added at $t = 2'$, and S -phase began 15 to 20' later. DNA replication was monitored by incorporating two different fluorescent dyes into the newly synthesized DNA. The first dye was added before the cell enters S -phase in order to label the entire genome. The second dye was added at successive time points $t = 25, 29, 32, 35, 39$, and $45'$, in order to label the later replicating DNA. DNA taken from each time point was combed, and measurements were made on replicated and unreplicated regions. The experimental details are described elsewhere (Herrick et al., 2000), but the approach is similar to DNA fiber autoradiography, a method that has been in use for the last 30 years (Huberman and Riggs, 1966; Jasny and Tamm, 1979). Indeed the same approach has recently been adapted to study the regulatory parameters of DNA replication in HeLa cells (Jackson and Pombo, 1998). Molecular combing, however, has the advantage that a large amount of DNA may be extended and aligned on a glass slide which ensures significantly better statistics (over several thousand measurements corresponding to several hundred genomes per coverslip). Indeed, the molecular combing experiments provide, for the first time, easy access to the quantities of data necessary for testing models such as the one

advanced in this paper.

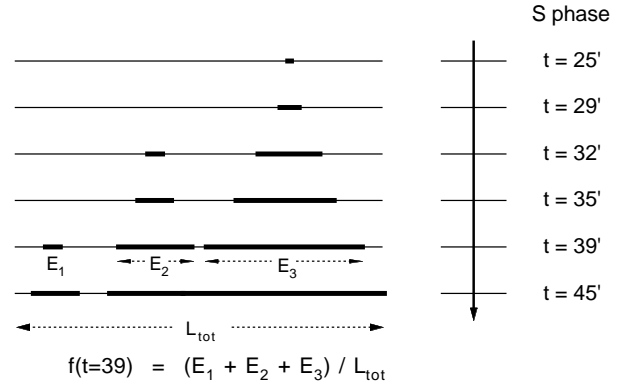


FIG. 1. Schematic representation of labeled and combed DNA molecules. Since replication initiates at multiple dispersed sites throughout the genome, the DNA can be differentially labeled, so that each linearized molecule contains alternating subregions stained with either one or both dyes. The thick segments correspond to sequences synthesized in the presence of a single dye (eyes). The thin segments correspond to those sequences that were synthesized after the second dye was added (holes). The result is an unambiguous distinction between eyes and holes (earlier and later replicating sequences) along the linearized molecules. Replication is assumed to have begun at the midpoints of the thick sequences (dotted lines) and to have proceeded bidirectionally from the site where DNA synthesis was initiated (arrows). Measurements between the centers of adjacent eyes provide information about replicon sizes (eye-to-eye distances). The fraction of the molecule already replicated by a given time, $f(\tau)$, is determined by summing the lengths of the thick segments and dividing that by the total length of the respective molecule.

Generalization of the simple version of the KJMA model

Analyzing the experimental results obtained on the kinetics of DNA replication in the *in vitro* cell-free system of *Xenopus laevis* (Herrick et al., 2000; Lucas et al., 2000), we found that the simple version of the crystal-growth model needed to be generalized in a number of ways:

1) Instead of assuming that the nucleation function $I(\tau)$ has the form $I(\tau) = I_0$ for $\tau \geq 0$, we allowed for an arbitrary form $I(\tau)$. Nucleation is believed to occur synchronously during the first half of S -phase in *Drosophila melanogaster* early embryos (Shinomiya and Ina, 1991; Blumenthal et al., 1974). Nucleation in the myxomycete *Physarum polycephalum*, on the other hand, occurs in

a very broad temporal window, suggesting that nucleation occurs continuously throughout *S*-phase (Pierron and Benard, 1996). Finally, recent observations suggest that in *Xenopus laevis*, early embryos nucleation may occur with increasing frequency as DNA synthesis advances (Herrick et al., 2000; Lucas et al., 2000). By choosing an appropriate form for $I(\tau)$, one can account for any of these scenarios. Below, we show how measured quantities may, using the model, be inverted to provide an estimate for $I(\tau)$.

2) The model assumes implicitly that the DNA analyzed began replication at $\tau = 0$, but this may not be so, for two reasons:

i) In the experimental protocols, the DNA analyzed comes from approximately 20,000 independently replicating nuclei. Before each genome can replicate, its nuclear membrane must form, along with, presumably, the replication factories. This process takes 15-20 minutes (Blow and Laskey, 1986; Blow and Watson, 1987; Wu et al., 1997). Because the exact amount of time can vary from cell to cell, the DNA analyzed at time t in the laboratory may have started replicating over a relatively wide range of times.

ii) In eukaryotic organisms, origin activation may be distributed in a programmed manner throughout the length of *S*-phase, and, as a consequence, each origin is turned on at a specific time (early and late) (Simon et al., 1999).

In the current experiment, the lack of information about the locations of the measured DNA segments along the genome means that we cannot distinguish between asynchrony due to reasons (i) or (ii). We can however account for their combined effects by introducing a starting-time distribution $\phi(t')$, which is the probability—for whatever reason—that a given piece of analyzed DNA began replicating at time t' in the lab. We assume that the distribution is Gaussian, with unknown mean and standard deviation, an assumption that will be justified by the fits to the data.

3) The models described above assumed that statistics could be calculated on infinitely long segments of DNA. In the experimental approach, the combed DNA is broken down into relatively short segments (200 kb, typically). Although it is difficult to account for this effect analytically, we wrote a Monte Carlo simulation that can mimic such “finite-size” effects. As we show below (Fig. 3D), we find evidence that there is no spatial variation in nucleation rates on scales *less* than 200 kb.

4) The experiments are all analyzed using an epifluorescence microscope to visualize the fluorescent tracks of

combed DNA on glass slides. The spatial resolution ($\approx 0.3 \mu\text{m}$) means that smaller signals will not be detectable. Thus, two replicated segments separated by an unreplicated region of size $< 0.3 \mu\text{m}$ will be falsely assumed to be one longer replicated segment. We accounted for this in the simulations by calculating statistics on a coarse lattice whose size equalled the optical resolution, while the simulation itself takes place on a finer lattice.

We can redo the analysis of the DNA kinetics for general $I(\tau)$. Eq. 1 then generalizes to

$$f(\tau) = 1 - e^{-g(\tau)}, \quad \text{with} \quad g(\tau) = 2v \int_0^\tau I(\tau')(\tau - \tau') d\tau', \quad (7)$$

and, similarly, Eq. 3 becomes

$$\ell_h(\tau) = \left[\int_0^\tau I(\tau') d\tau' \right]^{-1}. \quad (8)$$

The other mean lengths, $\ell_i(\tau)$ and $\ell_{i2i}(\tau)$, continue to be related to $\ell_h(\tau)$ by the general expressions given in Eqs. 4 and 5. In the experiment, one measures ℓ_h , ℓ_i , and ℓ_{i2i} as functions of both τ and f . (Because of the start-time ambiguity, the f data are easier to interpret.) The goal is to invert this data to find $I(\tau)$. Using Eqs. 7 and 8, we find

$$\tau(f) = \frac{1}{2v} \int_0^f \ell_{i2i}(f') df' = \frac{1}{2v} \int_0^f \frac{\ell_h(f')}{1 - f'} df'. \quad (9)$$

Because $\tau(f)$ increases monotonically, one can numerically invert it to find $f(\tau)$. From $f(\tau)$, one can derive all quantities of interest, including $I(\tau)$.

Using the generalizations discussed above, we analyzed recent results obtained on DNA replication in the *Xenopus laevis* cell-free system. DNA taken from each time point was combed, and measurements were made on replicated and unreplicated regions. Statistics from each time point were then compiled into four histograms (24 histograms for the 6 time points): $\rho(f, t)$, $\rho_h(\ell, t)$, $\rho_i(\ell, t)$, and $\rho_{i2i}(\ell, t)$, where ρ is the distribution of replicated fractions f at time t , ρ_h is the hole-length ℓ distributions at time t , etc. For reasons of space, only the $\rho(f, t)$ distributions are shown (Fig. 2).

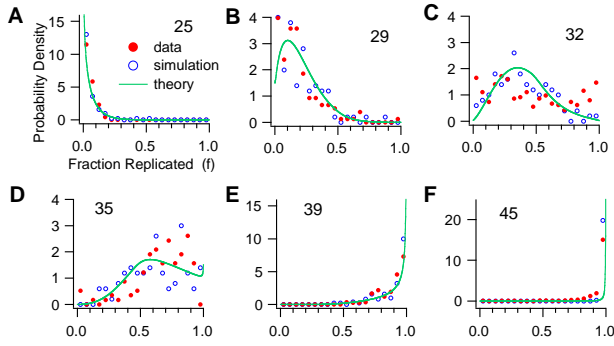


FIG. 2. $\rho(f, t)$ distributions for the 6 time points. The curves show the probability that a molecule at a given time point (A-F) has undergone a certain amount of replication before the second dye was added. The red points represent the experimental data. The results of the Monte Carlo simulation are shown in blue, analytical curves in green.

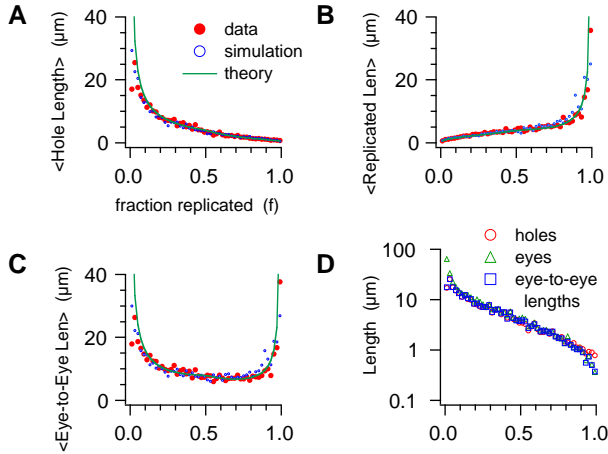


FIG. 3. Mean quantities vs. replication fraction. (A) $\ell_h(f)$; (B) $\ell_i(f)$; (C) $\ell_{i2i}(f)$. Red points are data; blue points are from the Monte-Carlo simulation; the green curve is a least-squares fit, based on a two-segment $I(\tau)$ and excluding data points larger than $10 \mu\text{m}$ (because of finite-size effects); (D) curves in (A)-(C) collapsed onto a single plot, confirming mean-field hypothesis. (The discrepancies near $f = 0$ and 1 reflect the added errors in measuring very small eyes or holes, because of optical-resolution limitations, or very large eyes or holes, because of finite-segment limitations.)

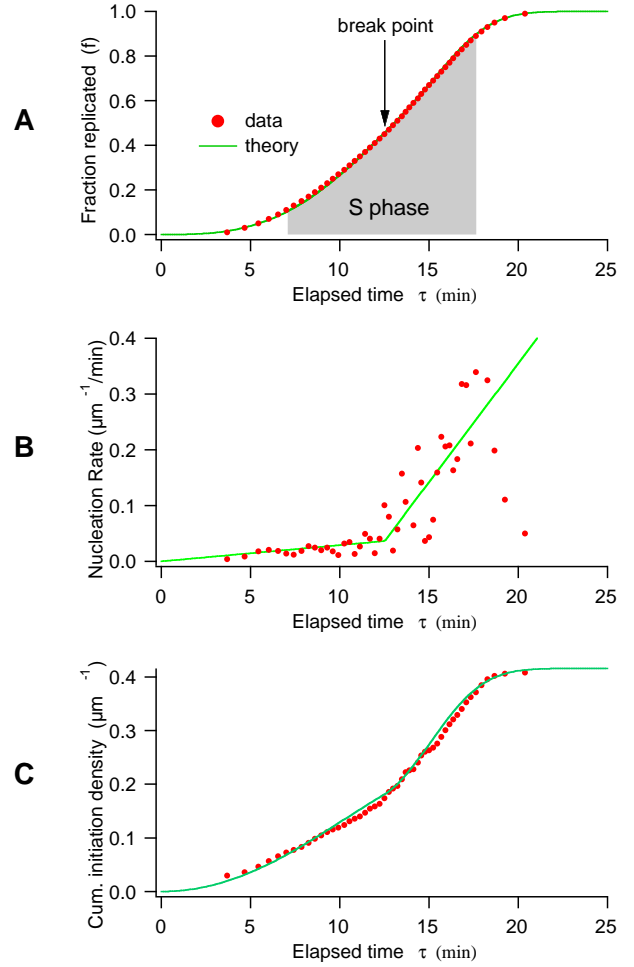


FIG. 4. (A) Fraction of replication completed, $f(\tau)$. Red points are derived from the measurements of mean hole, eye, and eye-to-eye lengths. Green curve is an analytic fit (see below). Shaded area runs from 10% to 90% replicated (10.5 min.) The time from the first origin initiation to the last coalescence is approximately 25 min. (B) Initiation rate $I(\tau)$. The large statistical scatter arises because the data points are obtained by taking two numerical derivatives of the $f(\tau)$ points in A. (C) Integrated origin separation, $I_{tot}(\tau)$, which gives the average distance between all origins activated up to time τ . In A-C, the green curves are from fits that assume that $I(\tau)$ has two linear regimes of different slopes. The form we chose for $I(\tau)$ was the simplest analytic form consistent with the data in B. The parameters for the least-squares fits (slopes I_1 and I_2 , break point τ_1) are obtained from a global fit to the three data sets in Fig. 3A-C, i.e., $\ell_h(f)$, $\ell_i(f)$, and $\ell_{i2i}(f)$.

One can immediately see from the distribution of replicated fractions $\rho(f, t)$ the need to account for the spread in starting times. If all the segments of DNA that were analyzed had started replicating at the same time, then the distributions would have been concentrated over a very small range of f . But, as one can see in Fig. 2C,

some segments of DNA (within the same time point) have already finished replicating ($f = 1$) before others have even started ($f = 0$). This spread is far larger than would be expected on account of the finite length of the segments analyzed.

Because of the need to account for the spread in starting times, it is simpler to begin by sorting data by the replicated fraction f of the measured segment. We thus assume that all segments with a similar fraction f are at roughly the same point in S -phase, an assumption that we can check by partitioning the data into subsets and redoing our measurements on the subsets. In Fig. 3A-C, we plot the mean values ℓ_h , ℓ_i , and ℓ_{i2i} against f . We then find $f(\tau)$, $I(\tau)$, and the cumulative distribution of lengths between activated origins of replication, $I_{tot}(\tau)$. (See Fig. 4.)

The direct inversion for $I(\tau)$ (Fig. 4b) shows several surprising features: First, origin activation takes place throughout S -phase and with increasing probability (measured relative to the amount of unreplicated DNA), as recently inferred by a cruder analysis of data from the same system using plasmid DNA (Lucas et al., 2000). Second, about halfway through S -phase, there is a marked increase in initiation rate, an observation that, if confirmed, would have biological significance. It is not known what might cause a sudden increase (break point) in initiation frequency halfway through S -phase. The increase could reflect a change in chromatin structure that may occur after a given fraction of the genome has undergone replication. This in turn may increase the number of potential origins as DNA synthesis advances (Pasero and Schwob, 2000).

The smooth curves in Fig 3A-C are fits based on the model, using an $I(\tau)$ that has two linearly increasing regions, with arbitrary slopes and “break point” (three free parameters). The fits are quite good, except where the finite size of the combed DNA fragments becomes relevant. For example, when mean hole, eye, and eye-to-eye lengths exceed about 10% of the mean fragment size, larger segments in the distribution for $\ell_h(f)$, etc., are excluded and the averages are biased down. We confirmed this with the Monte-Carlo simulations, the results of which are overlaid on the experimental data. The finite fragment size in the simulation matches that of the experiment, leading to the same downward bias. In Fig. 4, we overlay the fits on the experimental data. We emphasize that we obtain $I(\tau)$ directly from the data, with no fit parameters. The analytical form is just a model that summarizes the main features of the origin-initiation rate we determine via our model, from the experimental data. The important result is $I(\tau)$.

From the maximum of $I_{tot}(\tau)$, we find a mean spacing between activated origins of 4.8 ± 0.5 kb, which is much smaller than the minimum mean eye-to-eye separation 14 ± 1 kb. Interestingly, the former value agrees well with the calculated distribution of chromatin-bound

ORC molecules (Walter and Newport, 1997), while the mean eye-to-eye size coincides with the average chromatin loop size (Buongiorno et al., 1982; Blow and Chong, 1996). In our model, the two quantities differ if initiation takes place throughout S -phase, as coalescence of replicated regions leads to fewer domains (and hence fewer inferred origins). The mean eye-to-eye separation is of particular interest because its inverse is just the domain density (number of active domains per length), which can be used to estimate the number of active replication forks at each moment during S -phase. For example, the saturation value of I_{tot} corresponds to the maximum number (about 600,000/genome) of active origins of replication. Since there are about 400 replication foci/cell nucleus, this would indicate a partitioning of approximately 1,500 origins (or, equivalently, about 7.5 Mb) per replication focus (Blow and Laskey, 1986; Mills et al., 1989).

Because the distribution of f values in the $\rho(f, t)$ plots depends on the unknown starting-time distribution ($\phi(t')$), we used the parameters for $I(\tau)$ in order to derive the fork velocity v and the mean and width of the Gaussian form assumed for $\phi(t')$. As with the f data, we did a global fit to data from all six time points. We find $v = 640 \pm 40$ bases/min., in excellent agreement with previous estimates (Mahbubani et al., 1992; Lu et al., 1998).

One can test whether adding higher moments to the assumed Gaussian form significantly improves the fits, and, in our case, they do not. (Specifically, we added skewness and kurtosis, i.e., third and fourth moments.) This implies that the actual shape of the starting-time distribution does not differ greatly from a Gaussian form.

In a future experiment, it would be very desirable to obtain independent information about the form of $\phi(t)$. One could then constrain other parameters more tightly. For example, there is a high correlation between the mean starting time of molecules (here, 20.4 min.) and the velocity. (The width of the distribution, 2.6 min., is much less coupled in the fits.) An effect that might then be included in the model is a variable fork velocity. For example, v might decrease as forks coalesce or as replication factor becomes limiting toward the end of S phase (Blow and Laskey, 1986; Blow and Watson, 1987; Wu et al., 1997; Pierron and Benard, 1996). Such effects, if present, are small enough that they are difficult to see in the present case.

Another important question is to separate the effects of any intrinsic distribution due to early and late-replicating regions of the genome of a single cell from the extrinsic distribution caused by having many cells in the experiment. One approach would be to isolate and comb the DNA from a *single* cell. Although difficult, such an experiment is technically feasible. The latter problem could be resolved by *in situ* fluorescence observations of the chosen cell.

Finally, an implicit assumption of our analysis has been that there is no spatial organization in the nucleation origins—i.e., that $I(\tau)$ does not depend on the position x . Directly testing the mean-field hypothesis by the data collapse shown in Fig. 3D justifies this assumption on length scales up to 200 kb.

DISCUSSION

The view that we are led to here, of random initiation events occurring continuously during the replication of *Xenopus* sperm chromatin in egg extracts, is in striking contrast to what has until recently been the accepted view of a regular periodic organization of replication origins throughout the genome (Buongiorno et al., 1982; Laskey, 1985; Coverly and Laskey, 1994; Blow and Chong, 1996). For a discussion of experiments that raise doubts on such a view, see (Berezney, 2000). The application of our model to the results of Herrick et al. indicate that the kinetics of DNA replication in the *X. laevis in vitro* system closely resembles that of genome duplication in early embryos. Specifically, we find that the time required to duplicate the genome *in vitro* agrees well with what is observed *in vivo*. In addition, the model yields accurate values for replicon sizes and replication fork velocities that confirm previous observations (Mahbubani et al., 1992; Hyrien and Mechali, 1993). Though replication *in vitro* may differ biologically from what occurs *in vivo*, the results nevertheless demonstrate that the kinetics remains essentially the same. Of course, the specific finding of an increasing rate of initiation invites a biological interpretation involving a kind of autocatalysis, whereby the replication process itself leads to the release of a factor whose concentration determines the rate of initiation. This will be explored in future work.

One can entertain many further applications of the basic model discussed above, which can be generalized, if need be. For example, Blumenthal *et al.* interpreted their results on replication in *Drosophila melanogaster* for $\rho_{i2i}(\ell, f)$ to imply periodically spaced origins in the genome (Blumenthal et al., 1974). (See their Fig. 7.) It is difficult to judge whether their peaks are real or statistical happenstance, but one could check the mean-field hypothesis independently for that data. If the conclusion is indeed that the origins in that system are arranged periodically, the kinetics model could be generalized in a straightforward way (introducing an $I(x, \tau)$ that was periodic in x). Similar generalizations can be easily incorporated into the model to account for DNA replication in other organisms, including yeast and *Physarum*.

CONCLUSION

In this article, we have introduced a class of theoretical models for describing replication kinetics that is inspired by well-known models of crystal-growth kinetics. The model allows us to extract the rate of initiation of new origins, a quantity whose time dependence is has not previously been measured. With remarkably few parameters, the model fits quantitatively the most detailed existing experiment on replication in *Xenopus*. It reproduces known results (for example, the fork velocity) and provides the first reliable description of the temporal organization of replication initiation in a higher eukaryote. Perhaps most important, the model can be generalized in a straightforward way to describe replication and extract relevant parameters in essentially any organism.

ACKNOWLEDGMENTS

We thank M. Wortis and S. Jun for helpful comments and insights. This work was supported by grants from the Fondation de France, NSERCC, and NIH.

REFERENCES

- Avrami, M. 1939. Kinetics of Phase Change. I. General theory. *J. Chem. Phys.* 7:1103–1112. 1940. Kinetics of Phase Change. II. Transformation-time relations for random distribution of nuclei. *Ibid.* 8:212–224. 1941. Kinetics of phase change III. Granulation, phase change, and microstructure. *Ibid.* 9:177–184.
- Ben-Naim, E., and P. L. Krapivsky. 1996. Nucleation and growth in one dimension. *Phys. Rev. E* 54:3562–3568.
- Bensimon A., A. Simon, A. Chiffaudel, V. Croquette, F. Heslot, and D. Bensimon. 1994. Alignment and sensitive detection of DNA by a moving interface. *Science* 265:2096–2098.
- Berezney, R., D. D. Dubey, and J. A. Huberman. 2000. Heterogeneity of eukaryotic replicons, replicon clusters, and replication foci. *Chromosoma* 108:471–484.
- Blow, J. J., and J. P. Chong. 1996. DNA replication in *Xenopus*. In *DNA Replication in Eukaryotic Cells*. Cold Spring Harbor Laboratory Press, Cold Spring Harbor. 971–982.
- Blow, J. J., and R. A. Laskey, 1986. Initiation of DNA replication in nuclei and purified DNA by a cell-free extract of *Xenopus* eggs. *Cell* 47:577–587.
- Blow, J. J., and J. V. Watson. 1987. Nuclei act as independent and integrated units of replication in a *Xenopus* cell-free DNA replication system. *Embo J.* 6:1997–2002.
- Blumenthal, A. B., H. J. Kriegstein, and D. S. Hogness. 1974. The units of DNA replication in *Drosophila melanogaster* chromosomes. In *Cold Spring Harbor Symposia on Quantitative Biology*. 38:205–223.
- Brewer, B. J., and W. L. Fangman. 1993. Initiation at Closely Spaced Replication Origins in a Yeast Chromosome. *Science* 262:1728–1731.
- Buongiorno-Nardelli, M., G. Michelli, M. T. Carri, and M. Marilley. 1982. A relationship between replicon size and supercoiled loop domains in the eukaryotic genome. *Nature* 298:100–102.
- Cahn, J. W. 1996. Johnson-Mehl-Avrami Kinetics on a Finite Growing Domain with Time and Position Dependent Nucleation and Growth Rates. *Mat. Res. Soc. Symp. Proc.* 398:425–438.
- Cairns, J. 1963. The Chromosome of *E. coli*. In *Cold Spring Harbor Symposia on Quantitative Biology*. 28:43–46.
- Christian, J. W. 1981. The Theory of Phase Transformations in Metals and Alloys, Part I: Equilibrium and General Kinetic Theory. Pergamon Press, New York.
- Coverley, D. and R. A. Laskey. 1994. Regulation of eukaryotic DNA replication. *Ann. Rev. Biochem.* 63:745–776.
- Friedman, K. L., B. J. Brewer, and W. L. Fangman. 1997. Replication profile of *Saccharomyces cerevisiae* chromosome VI. *Genes to Cells* 2:667–678.
- Gomez, M., and F. Antequera. 1999. Organization of DNA replication origins in the fission yeast genome. *EMBO J.* 18:5683–5690.
- Hand, R. 1978. Eukaryotic DNA: organization of the genome for replication. *Cell* 15:317–325.
- Herrick, J., X. Michalet, C. Conti, C. Schurra, and A. Bensimon. 2000. Quantifying single gene copy number by measuring fluorescent probe lengths on combed genomic DNA. *Proc. Natl. Acad. Sci. USA* 97:222–227.
- Herrick, J., P. Stanislawski, O. Hyrien, and A. Bensimon. 2000. A novel mechanism regulating DNA replication in *Xenopus laevis* egg extracts. *J. Mol. Biol.* 300:1133–1142.
- Huberman, J. A., and A. D. Riggs. 1966. Autoradiography of chromosomal DNA fibers from Chinese hamster cells. *Proc. Natl. Acad. Sci. USA* 55:599–606.
- Hyrien, O. and M. Mechali 1993. Chromosomal replication initiates and terminates at random sequences but at regular intervals in the ribosomal DNA of *Xenopus* early embryos. *EMBO Journal* 12:4511–4520.
- Jackson, D. A., and A. Pombo. 1998. Replication Clusters Are Stable Units of Chromosome Structure: Evidence That Nuclear Organization Contributes to the Efficient Activation and Propagation of S Phase in Human Cells. *J. Cell Biol.* 140:1285–1295.
- Jasny, B. R., and I. Tamm. 1979. Temporal organization of replication in DNA fibers of mammalian cells. *J. Cell Biol.* 81:692–697.
- Johnson, W. A., and P. A. Mehl. 1939. *Trans. AIMME*. 135:416–442. Discussion 442–458.
- Kolmogorov, A. N. 1937. On the statistical theory of crystallization in metals. *Izv. Akad. Nauk SSSR, Ser. Fiz.* 1:355–359.

- Laskey, R. A. 1985. Chromosome replication in early development of *Xenopus laevis*. *J. Embryology & Experimental Morphology*. 89, Suppl:285–296.
- Lu, Z. H., D. B. Sittman, P. Romanowski, and G. H. Leno. 1998. Histone H1 reduces the frequency of initiation in *Xenopus* egg extract by limiting the assembly of prereplication complexes on sperm chromatin. *Mol. Biol. of the Cell*. 9:1163–1176.
- Lucas, I., M. Chevrier-Miller, J. M. Sogo, and O. Hyrien. 2000. Mechanisms Ensuring Rapid and Complete DNA Replication Despite Random Initiation in *Xenopus* Early Embryos. *J. Mol. Biol.* 296:769–786.
- Mahbubani, H. M., T. Paull, J. K. Elder, and J. J. Blow. 1992. DNA replication initiates at multiple sites on plasmid DNA in *Xenopus* egg extracts. *Nucl. Acids Res.* 20:1457–1462.
- Michalet X., R. Ekong, F. Fougerousse, S. Rousseaux, C. Schurra, N. Hornigold, M. van Slegtenhorst, J. Wolfe, S. Povey, J. S. Beckmann, and A. Bensimon. 1997. Dynamic molecular combing: stretching the whole human genome for high-resolution studies. *Science*. 277:1518–1523.
- Mills, A. D., J. J. Blow, J. G. White, W. B. Amos, D. Wilcock, and R. A. Laskey. 1989. Replication occurs at discrete foci spaced throughout nuclei replicating in vitro. *J. Cell Sci.* 94:471–477.
- Pasero, P., and E. Schwob. 2000. Think global, act local - how to regulate S phase from individual replication origins. *Current Opinion in Genetics and Development*. 10:178–186.
- Pierron, G., and M. Benard. 1996. DNA Replication in *Physarum*. In *DNA Replication in Eukaryotic Cells*. M. DePamphilis, ed. Cold Spring Harbor Laboratory Press, Cold Spring Harbor. 933–946.
- Plischke, M., and B. Bergersen. 1994. Equilibrium Statistical Physics, 2nd ed., Ch. 3. World Scientific, Singapore.
- Sekimoto, K. 1991. Evolution of the domain structure during the nucleation-and-growth process with non-conserved order parameter. *Int. J. Mod. Phys. B* 5:1843–1869.
- Shinomiya, T., and S. Ina. 1991. Analysis of chromosomal replicons in early embryos of *Drosophila melanogaster* by two-dimensional gel electrophoresis. *Nucleic Acids Research*. 19:3935–3941.
- Shivashankar, G. V., M. Feingold, O. Krichevsky, and A. Libchaber. 1999. RecA polymerization on double-stranded DNA by using single-molecule manipulation: The role of ATP hydrolysis. *Proc. Natl. Acad. Sci. USA*. 96:7916–7921.
- Simon, I., T. Tenzen, B. E. Reubinoff, D. Hillman, J. R. McCarrey, and H. Cedar. 1999. Asynchronous replication of imprinted genes is established in the gametes and maintained during development. *Nature*. 401:929–932.
- Walter, J., and J. W. Newport. 1997. Regulation of replicon size in *Xenopus* egg extracts. *Science*. 275:993–995.
- Wu, J. R., G. Yu, and D. M. Gilbert. 1997. Origin-specific initiation of mammalian nuclear DNA replication in a *Xenopus* cell-free system. *Methods*. 13:313–324.